Dissociation of Bacteriophage T4 DNA Polymerase and Its Processivity Clamp after Completion of Okazaki Fragment Synthesis†

Theodore E. Carver, Jr.,‡ Daniel J. Sexton, and Stephen J. Benkovic*

Department of Chemistry, 152 Davey Laboratory, The Pennsylvania State University, University Park, Pennsylvania 16802

Received June 13, 1997; Revised Manuscript Received October 1, 1997⊗

ABSTRACT: The mechanism of bacteriophage T4 DNA polymerase (gp43) and clamp (gp45) protein dissociation from the holoenzyme•DNA complex was investigated under conditions simulating the environment encountered upon completion of an Okazaki fragment. Lagging strand DNA synthesis was approximated using a synthetic construct comprised of a doubly biotinylated, streptavidin-bound 62-mer DNA template, paired with complementary primers to generate an internal 12-base gap where the 5′-end primer contained either a 5′-OH (DNA primer) or a 5′-triphosphate (RNA primer) group. Rapid kinetic measurements revealed that upon encountering the blocking primer, the holoenzyme either dissociates from DNA (∼40%) or strand-displaces the blocking strand (∼60%). The two blocking oligonucleotides (DNA or RNA) induce a 30−50-fold increase in the rate of holoenzyme dissociation, with both polymerase and clamp proteins dissociating simultaneously. Inhibition of ATP hydrolysis by ATP-γ-S did not have a measurable effect upon holoenzyme dissociation from DNA. The presence of gp32, the single-strand binding protein, caused a small (3-fold) increase in the rate constant for dissociation.

Organisms with genomes greater than several kilobases require both continuous (leading) and discontinuous (lagging) modes of DNA replication to efficiently copy their genetic information. In bacteriophage T4, a single DNA polymerase holoenzyme is responsible for both leading and lagging strand DNA synthesis (*1*). This holoenzyme is a multisubunit complex consisting of the polymerase subunit (gp43)[1] and a trimeric processivity clamp (gp45), which is catalytically loaded onto DNA by the clamp loader (gp44/62) (*2*, *3*). The properties of the ATP-dependent clamp loader have been described in detail elsewhere (*4*−*6*). A helicase (gp41/59) unwinds DNA in advance of the leading strand DNA polymerase, and a primase (gp61), acting in concert with the helicase, synthesizes the RNA primers used to prime lagging strand DNA synthesis. Lastly, a single-stranded DNA binding protein (gp32) coats single-stranded regions that are formed as the helicase unwinds DNA in front of the replication fork.

Lagging strand DNA synthesis involves the repetitive generation of short RNA primers followed by their extension into Okazaki fragments, which are hundreds to thousands of bases in length. The process of defining the minimal elements required for both leading and lagging strand DNA replication has been accomplished in the laboratories of Alberts and Nossal (*1*, *7*). Although the components are identified, the mechanism by which leading and lagging strand syntheses are coordinated is not understood. It is known from *in vitro* experiments and electron microscopic imaging that the activities of the lagging strand polymerase and the primase/helicase complex are coordinated (*1*, *7*, *8*), although the nature of the interactions defining this relationship remains unclear.

A minimal system containing the components required for lagging strand DNA synthesis is shown in Figure 1. There are three phases to lagging strand DNA synthesis: assembly of the polymerase holoenzyme, extension of the Okazaki fragment, and release of the polymerase at the end of the fragment. Since lagging strand DNA synthesis occurs processively, it is presumed that the lagging strand polymerase requires the same processivity clamp used for leading strand DNA synthesis (Figure 1A). The gp45 clamp is loaded catalytically onto DNA by the gp44/62 clamp loader (not shown), which also chaperones the T4 polymerase into a functional holoenzyme complex (*4*, *9*). During the extension phase of the reaction (Figure 1B), the fully assembled lagging strand holoenzyme generates products [average length = 1000−2000 bp (*8*)] at an undetermined rate. However, using the known rates of multiple base incorporation with the isolated polymerase subunit, a half-time of ≈5−10 s for the completion of an Okazaki fragment can be calculated (*10*). This extension time does not include the time required for RNA primer synthesis by the primase. The final stage of lagging strand synthesis is termination at the 5′ end of the previous Okazaki fragment (Figure 1C), at which point the holoenzyme is released. Hacker and Alberts (*11*) have shown that DNA synthesis is terminated rapidly when a G/C-rich hairpin in M13 DNA is encountered, suggesting that the holoenzyme is destabilized by the end of an Okazaki fragment.

Dilution and challenge experiments indicate that very low concentrations of the T4 replication proteins are sufficient to complete both leading and lagging strand DNA synthesis (*8*, *12*). The insensitivity of lagging strand DNA synthesis to dilution implies that each polymerase is continuously recycled, as opposed to a mechanism wherein a new DNA polymerase is recruited to extend each successive Okazaki

† Supported by National Institutes of Health Grants GM13306 (S.J.B.) and GM15729 (T.E.C.).

* Author to whom correspondence should be addressed.

‡ Present address: Argonne National Laboratory, Argonne, IL.

⊗ Abstract published in *Advance ACS Abstracts,* November 15, 1997.

[1] Abbreviations: IANBD, *N*-[(2-(iodoacetoxy)ethyl)-*N*-methyl]amino-7-nitrobenz-2-oxa-1,3-diazole; PCNA, proliferating cell nuclear antigen; bp, base pair; gp, gene product.

S0006-2960(97)01423-2 CCC: $14.00

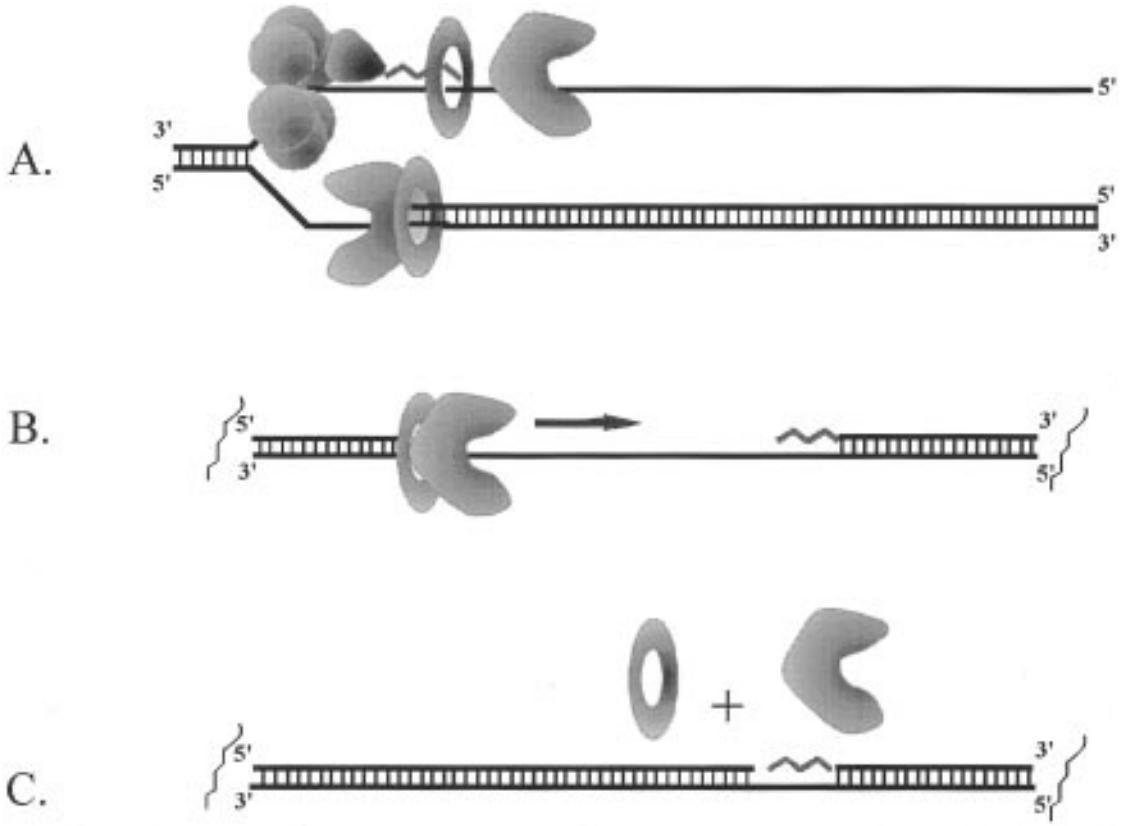

FIGURE 1: Initiation and termination of lagging strand DNA synthesis: (A) the processivity clamp (45) and the polymerase subunit are assembled onto a newly synthesized RNA primer at the T4 replication fork; (B) the polymerase holoenzyme performs DNA synthesis for hundreds to thousands of bases; (C) termination of Okazaki fragment synthesis occurs when the polymerase encounters the 5′ end of the penultimate fragment, and the polymerase subunit and its clamp are then released by an unknown mechanism, making them available for the next round of lagging strand DNA synthesis.

fragment. If the holoenzyme is recycled, then lagging strand DNA synthesis is dependent upon the time required for dissociation and recycling of a holoenzyme following successful completion of an Okazaki fragment. Slow dissociation would markedly inhibit the overall rate of DNA replication, because leading and lagging strand synthesis proceed at the same rate, and leading strand syntheses is probably halted prior to the start of a new Okazaki fragment (*13*). In the cycle of Okazaki fragment synthesis, the holoenzyme assembly and extension steps occur in <20 s, and optimal termination of lagging strand synthesis should occur on a similar time scale to facilitate recycling of the holoenzyme. A stalled holoenzyme is quite stable, with a half-life of 1−4 min, indicating that a more efficient dissociation mechanism is required to ensure rapid dissociation of the holoenzyme at the end of an Okazaki fragment (*4*, *14*).

A short, defined primer template has been used to study the kinetic mechanisms of holoenzyme assembly and function (*15*). In those experiments, it was shown that physical barriers, composed of either streptavidin or a DNA fork at the end of the substrate, are required to prevent the rapid dissociation of the circular trimeric clamp from the ends of DNA. In this paper, we use a similar 62-mer template containing biotin/streptavidin blocks on both ends to facilitate assembly of the holoenzyme (Figure 2). This template was designed to contain a downstream DNA sequence employed by T4 to initiate Okazaki fragment synthesis. We paired this template with 17-mer and 36-mer DNA and RNA oligonucleotides, generating a 12 base single-strand DNA gap. The resulting DNA substrate simulates an actual Okazaki fragment that is near completion. This substrate was used in several assays designed to examine the mechanisms of polymerase and trimeric clamp dissociation under different conditions and to define the substrate requirements for Okazaki fragment termination in bacteriophage T4.

EXPERIMENTAL PROCEDURES

Materials. Oligonucleotides were synthesized with an Expedite 8909 DNA synthesizer (Perceptive Biosystems) and purified according to the method of Capson *et al*. (*10*). Biotin-labeled oligonucleotides were prepared using the BioTEG phosphoramidite and BioTEG CPG obtained from Glen Research. ATP-γ-S was purchased from Boehringer Mannheim as a 98% pure solution and used without further purification. T4 polynucleotide kinase (United States Biochemical) was used to 5′-end-label oligonucleotides with [γ-^{32}P]ATP (New England Nuclear). All other chemicals were obtained from Sigma or Fisher Scientific and were of analytical grade or better.

Protein Preparations. The wild type 45 protein and the 44/62 complex were purified from *Escherichia coli*, as previously described, using expression vectors obtained from Dr. William Konigsberg (Yale University) (*16*). The T7C-45 protein was purified in the same manner but was expressed in *E. coli* using an expression vector obtained from Dr. John Kuriyan (Rockefeller University). The preparation of the ANBD fluorescently labeled T7C mutant of the 45 protein was previously described (*17*). The T4 exonuclease-deficient polymerase D219A mutant was purified as described (*18*) and used in all of the following experiments to

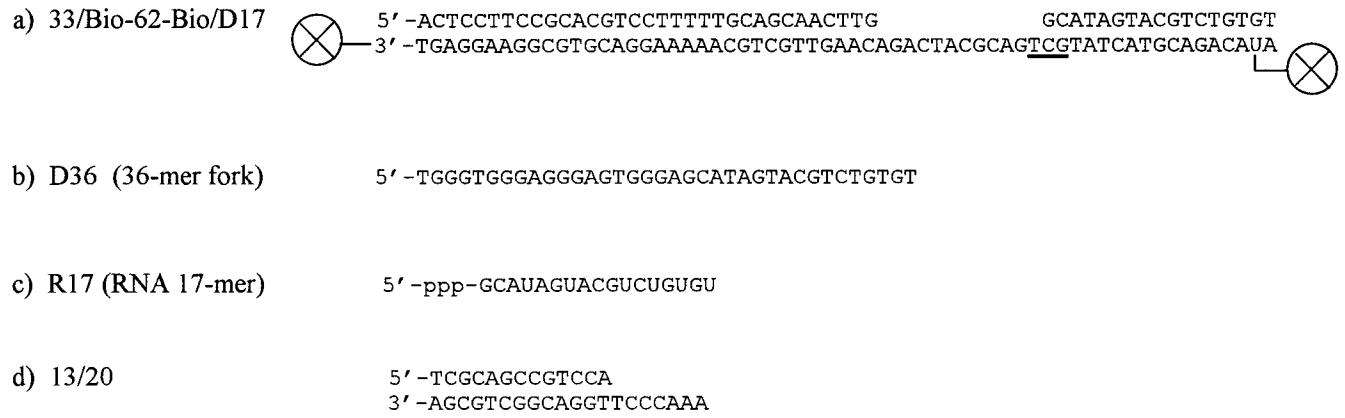

FIGURE 2: Substrates used to study termination of Okazaki fragment synthesis: (a) the 33/Bio-62-Bio/D17 contains a 17-mer DNA oligonucleotide to block extension from a 33-mer primer [the T4 primase recognition site (3′TCG5′) is underscored; (b) 36-mer DNA used to assemble a fork downstream from the DNA primer; (c) 17-mer RNA used to mimic the 5′ end of an RNA primer; (d) 13/20-mer substrate used as a trap to monitor release of the polymerase subunit.

avoid complications arising from the presence of the exonuclease activity. The polymerase activity of the T4 D219A polymerase is identical to that of the wild type enzyme (*18*).

Primer-Template Construction. The biotinylated 33/62 DNA substrate was constructed by ligation of a 3′-biotinylated 23-mer and a 5′-biotinylated 39-mer using a previously described ligation method (*9*). The product of the ligation reaction consisted of a 33-mer primer annealed to a 62-mer template containing biotins attached through linkers at both ends. Alternatively, the doubly biotinylated 62-mer oligonucleotide was synthesized directly on a Perseptive Biosystems Expedite 8909 oligonucleotide synthesizer. The 33/62 primer templates were purified by nondenaturing polyacrylamide gel electrophoresis and quantitated using incorporation of [α-^{32}P]dATP by Klenow fragment followed by filter binding and scintillation counting as described previously (*15*). This method of quantitation ensures that the reported substrate concentrations correspond to the concentration of properly annealed, extendable primers. This primer-template was then annealed with a 20% excess of a blocking oligonucleotide complementary to the 5′ end of the template, generating a 12-base gap (Figure 2). To verify that the blocking oligonucleotides were quantitatively annealed to their respective templates, extension reactions were performed using the nonprocessive polymerase subunit (gp43). This assay required many turnovers (>5 min) before strand displacement products began to accumulate, demonstrating that >90% of the primer-template/block substrates were fully annealed. For experiments employing a 17-mer RNA oligonucleotide, RNA was synthesized enzymatically using T7 RNA polymerase and a 17/34 primer template containing the T7 promoter recognition sequence. The final product of this reaction, containing the correct complementary sequence and a triphosphorylated 5′ terminus, was purified by denaturing polyacrylamide gel electrophoresis in the presence of 8 M urea, under RNase-free conditions. The integrity of the 17-mer RNA triphosphate was verified by a gel shift assay that compared electrophoretic mobilities of the RNA before and after partial digestion with shrimp alkaline phosphatase (data not shown). For some experiments, enzymatic RNA synthesis was performed in the presence of [α-^{32}P]UTP, generating a radiolabeled product. No RNA degradation by the assembled holoenzyme was evident by gel electrophoresis, which contrasts with reports of degradation by the gp43 polymerase alone (*19*).

Assay for Turnover of 13/20-mer following Release of Polymerase. An indirect assay for extension of ^{32}P-5′-end-labeled 13/20-mer was used for the initial characterization of the holoenzyme dissociation reaction. An assay mixture containing 150 nM 34/62/36-mer DNA, 120 nM streptavidin, and 1 mM ATP was incubated for 30 s with 100 nM T4 D219A polymerase, 150 nM 44/62 complex, and 150 nM 45 protein (trimer) and subsequently mixed with a solution containing either three deoxynucleotides (dATP, dCTP, dGTP) or all four deoxynucleotides (80) μM each, final concentration) and the 13/20-mer substrate (2 μM final concentration) in complex buffer (25 mM Tris-acetate, pH 7.4, 150 mM potassium acetate, 10 mM magnesium acetate, and 10 mM β-mercaptoethanol) at 25 °C. At various times following mixing, aliquots were removed and quenched with 250 mM EDTA. The samples were then mixed with loading buffer and electrophoresed on an 8 M urea/16% polyacrylamide gel. As described previously, products of the extension reaction from the 13/20-mer were quantitated using a Molecular Dynamics phosphorimaging apparatus (*9*).

Rapid Quench Measurements of Strand Displacement by the Polymerase Holoenzyme. For real-time measurements of strand displacement, rapid quench mixing experiments were performed using a KinTek rapid quench apparatus (*20*, *21*). A sample containing 250 nM radiolabeled DNA primer template, 300 nM streptavidin, 200 nM polymerase subunit, 250 nM 45 and 44/62 proteins, and 1 mM ATP was mixed against dCTP, dGTP, dATP, dTTP, and sheared salmon sperm single-strand DNA trap (2 mg/mL) in complex buffer. Time points were collected in Eppendorf tubes, quenched in 2 M HCl, neutralized with 3 M NaOH/1 M Tris, and extracted with phenol/chloroform/isoamyl alcohol (25:24:1). The zero point was obtained by omitting the protein from the assay mixture. The samples were then mixed with loading buffer, electrophoresed on an 8 M urea/16% polyacrylamide gel, and quantitated using the Molecular Dynamics phosphorimaging apparatus. We note that stoichiometric mixing of the polymerase, accessory proteins, and primer template prevents 40−50% of the DNA substrate from being polymerized. This fraction is due to incorrectly assembled holoenzyme that is unable to perform DNA synthesis (*4*).

Our substrate includes a weak pause site that was documented previously (*9*). This site results in the accumulation of a 43-mer product at early and long times during the strand displacement reaction, independent of the

Scheme 1

$$S \xrightarrow{k_{BL}} P_{BL}$$

$$S \xrightarrow{k_{SD}} P_{SD}$$

presence of a blocking oligonucleotide (Figure 5). The 43-mer product observed at short times corresponds to transiently paused polymerase holoenzymes, whereas the appearance of this product at long times reflects a small portion of free polymerase that was not completely trapped by salmon sperm DNA after dissociating from the primer template. Thus, the absence of this product during the strand displacement reaction serves as an internal control to ensure that none of the blocked products are due to recycling of inefficiently trapped polymerase molecules.

Steady-State Fluorescence Emission Spectra. Steady-state fluorescence measurements were performed using a SLM Aminco 8000C photon counting spectrofluorometer equipped with a thermostated cell compartment that was maintained at 25 °C. Excitation and emission slit widths were each maintained at 4 nm.

Stopped-Flow Measurements of Trimeric Clamp Dissociation from the Assembled Holoenzyme Complex. The 33/62/17 substrates were complexed with a holoenzyme containing a fluorescently labeled processivity clamp. The T7C mutant of the gp45 clamp protein was labeled with *N*-[(2-(iodoacetoxy)ethyl)-*N*-methyl]amino-7-nitrobenz-2-oxa-1,3-diazole (IANDB) as described previously (*17*). The DNA primer template (250 nM) was combined with 300 nM streptavidin, the gp43, gp45, and gp44/62 proteins (250 nM each), and 100 μM ATP in complex buffer. The assembled holoenzyme complex was then mixed with glucose (20 mM) and glucose hexokinase (20 units/mL) to convert all remaining adenosine triphosphate to the diphosphate form. This mixture was immediately transferred to a stopped-flow instrument (Applied Photophysics), rapidly combined with all four nucleotides, and monitored over time by fluorescence changes as the labeled clamp dissociated from DNA.

Data Analysis. Under the conditions of our rapid quench experiment, the polymerase holoenzyme rapidly extended across the 12-base gap to form 45- and 46-mer products, paused, then either dissociated from this "blocked" product or strand displaced to form full-length extension products. The data were fitted to the single-exponential function $P_{BL} = S \exp(-k_{obs}t) + P_{BL\alpha}$, where $P_{BL\alpha}$ corresponded to the product that had not been converted to the strand-displaced form at long time. We analyzed these decays in terms of a model wherein a single paused intermediate (S) decays exponentially to two kinds of products, the dissociated blocked products (P_{BL}) and the strand displacement product (P_{SD}), with corresponding rate constants for each process (Scheme 1). The observed rate constant for the decay of S was given by $k_{obs} = k_{BL} + k_{SD}$. The individual rate constants were calculated using the expressions $k_{BL} = k_{obs}(F_{BL})$ and $k_{SD} = k_{obs}(1 - F_{BL})$, where F_{BL} is the fraction of the blocked product remaining at long times.

For all stopped-flow experiments, the observed time courses were fit to a single exponential plus offset, $y = A \exp(-kt) + C$, where A is the amplitude of the fluorescence decay, k is the rate constant for clamp dissociation, and C is the fluorescence offset. In some cases, a small (10−25%) fast phase was observed with a rate >3 s^{-1}. The fast phase was attributed to a small amount of association between the free gp45 and gp44/62 proteins, due to the ability of gp44/62 to use dATP as a substrate for the clamp loading reaction (*22*). This component was ignored because its amplitude was small, variable, and not present in most reactions using this substrate, whereas the fitted phase had a consistent rate and amplitude. Error estimates were derived from three or more independent experimental determinations.

RESULTS

Model System for Studying Termination of Lagging Strand Replication. We have used a short, defined primer-template system as a biochemical model for lagging strand DNA synthesis. This model is the first to incorporate several features that may be required for optimal termination of Okazaki fragments. Our substrate contains a fully paired, exposed 5′ terminus that is annealed opposite to a T4 primase recognition site (Figure 2). This short linear substrate was used to measure directly the dissociation of both the polymerase and its accessory processivity clamp using either rapid quench or stopped-flow fluorescence. The stopped-flow assay enabled us to examine the fate of the processivity clamp following dissociation of the polymerase subunit from a primer-template. In a previous study, Hacker and Alberts (*11*) used a primer extension assay to demonstrate that a hairpin in M13 DNA induced rapid dissociation, rather than stalling, of the T4 polymerase gp43 subunit. However, the M13 hairpin contains a unique, highly thermostable G/C-rich sequence that is markedly different from the 5′ end of an Okazaki fragment formed *in vivo*. Our study employed 33/62/D17 and 33/62/R17 substrates (Figure 2) to investigate factors that promote holoenzyme dissociation at the 5′ ends of Okazaki fragments.

Rapid Release of a Large Fraction of the Gp43 Protein from the Holoenzyme Complex following Polymerase Extension. When the polymerase is allowed to fully extend an excess of doubly biotinylated substrate, the initial reaction is much faster than subsequent turnovers, implying that the polymerase is limited by a slow rate of release when it encounters a biotin/streptavidin block (B. F. Kaboord and S. J. Benkovic, unpublished results). We sought to confirm that a substantial fraction of the polymerase molecules is released during extension on the gapped substrate. First, we demonstrated that the holoenzyme fills in the gap in our DNA construct when provided with all four nucleotides (data not shown). To monitor the release of the polymerase from a gapped primer-template, we included a large excess of a ^{32}P-labeled 13/20-mer trap in the reaction mixture. Prior to the start of the experiment, the polymerase holoenzyme was assembled on the 33/62/17-mer substrate containing a DNA block in the presence of ATP. The holoenzyme·DNA complex was then mixed with either three or four deoxynucleotides in the presence of excess 13/20-mer. When supplied with only three dNTPs, the polymerase stalls before completing synthesis of the gap, and turnover of the 13/20 trap is very slow, occurring on a time scale of minutes (Figure 3). This turnover rate is consistent with the long half-life of the T4 holoenzyme previously reported (*15*). However, when the polymerase is supplied with a complete set of four deoxynucleotides, the 13/20-mer trap is turned over to 14-mer and larger products in <30 s, indicating that a large fraction of polymerase has been released after

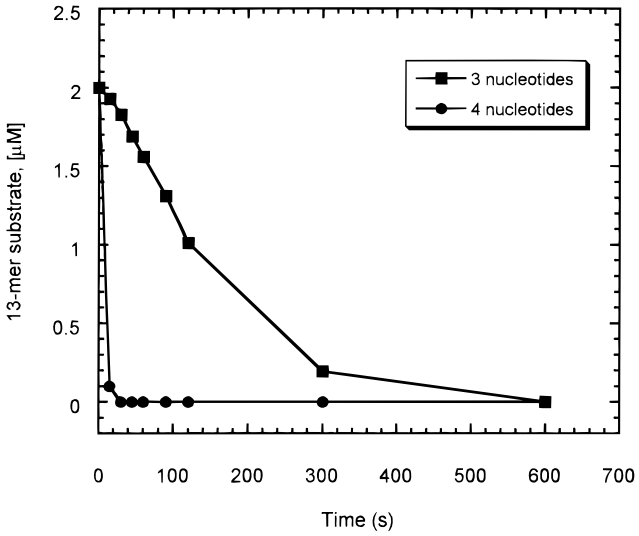

FIGURE 3: Turnover of the 13/20-mer trap following dissociation of polymerase holoenzymes assembled on the 33/62/D17 substrate: (■) holoenzyme supplied with dCTP, dGTP, and dTTP, causing the primer to be extended only four bases; (●) holoenzyme supplied with all four dNTPs. Conditions are described under Experimental Procedures.

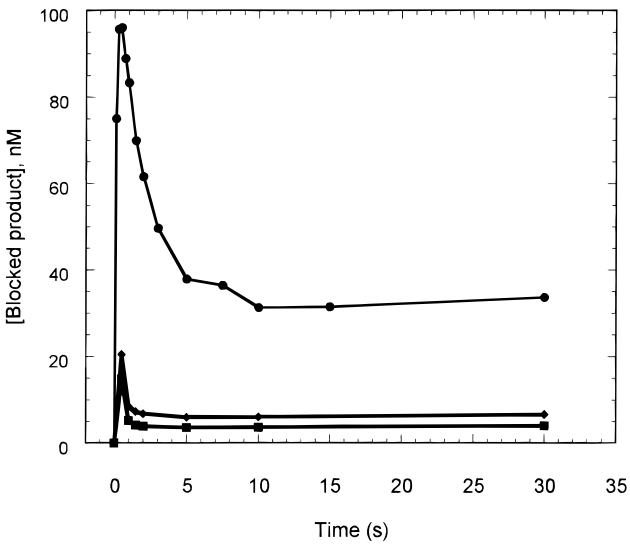

FIGURE 4: Effects of forked vs gapped substrates upon the products of the rapid quench extension reaction. Substrates: (●) 33/62/D17 (gapped substrate); (■) 33/62/D36 (forked substrate); (◆) 33/62 (primer-template with no blocking oligonucleotide). For each trace, the symbols represent actual data points generated by integration of radiolabeled products on a gel, connected by lines within each data set. Conditions are described under Experimental Procedures.

extension across a gap. This result suggests that a substantial fraction of the polymerase dissociates, rather than stalls, after performing gap-filling synthesis. Since the trap turnover rate is complicated by several factors unrelated to polymerase dissociation, we further characterized the products of the extension reaction using radiolabeled 33/62/17 primer-templates.

S*trand Displacement of a Forked Substrate versus Stalling and Dissociation on a Gapped Substrate*. To examine the products formed during extension across the gap, we analyzed the extension of labeled 33/62/17 substrates in a rapid chemical quench apparatus. These experiments were performed in the presence of a large excess of sheared salmon sperm DNA trap to prevent rebinding of the polymerase following dissociation. It has been previously shown that short forked substrates undergo strand displacement in <10 s (*15*). We examined the time course for strand displacement using either a forked substrate (33/62/36), a substrate containing a gap formed by a fully paired blocking oligonucleotide (33/62/D17), or a 33/62-mer with no blocking duplex region (Figure 2). For the forked substrate, there was no accumulation of intermediate blocked products (45-mer and 46-mer), consistent with a rate of strand displacement that is similar in magnitude to the unhindered polymerization rate constant of at least $50-100$ s^{-1} (*4*). In contrast, a fully paired 17-mer caused the holoenzyme to stall after extending across the gap, indicating that the holoenzyme quantitatively pauses upon encountering the nonfrayed 5′ end of an annealed oligonucleotide. After pausing, a fraction of the paused product is extended to 58-mer and 59-mer in a monophasic exponential decay, whereas the remainder forms a plateau at long times (Figure 4). We interpret this plateau in terms of a branched pathway, wherein ∼40% of the holoenzyme molecules rapidly dissociate and ∼60% are able to continue strand displacement DNA synthesis. In the resulting kinetic scheme, the k_{obs} for strand displacement synthesis is the sum of the rate constants for both strand displacement and dissociation (Scheme 1; Table 1). Thus, the holoenzyme can rapidly strand displace a duplex containing an unpaired flap; in contrast, a fully paired duplex induces its stalling and dissociation.

Effects of Blocking Oligonucleotide 5′ Structure on Holoenzyme Dissociation. The effects of the structure of a 5′ end of an Okazaki fragment were examined by comparing the rate of holoenzyme dissociation from DNA/DNA (33/62/D17) and RNA/DNA (33/62/R17) gapped substrates. The 33/62/R17 substrate contained a triphosphate on the 5′ end of the 17-mer RNA reproducing the 5′ end of an Okazaki fragment prior to processing by RNase H. A rapid chemical quench apparatus was used to measure the products formed after collision by extension into either a DNA block (33/62/D17) or an RNA block (33/62/R17). The products of these reactions were then separated by denaturing polyacrylamide gel electrophoresis and quantitated. Figure 5 shows the products of the extension of the 33/62/D17-mer primer-template containing a 17-mer DNA block. The reaction proceeded by complete extension of the 33-mer to a 46-mer and was followed by subsequent strand displacement of a fraction of the blocked product. Interestingly, the 46-mer stalled product was formed by displacing one nucleotide (deoxyguanosine) from the 5′-terminal end of the DNA or RNA block (Figure 2). We found that the RNA block induced a $2-3$-fold faster rate of dissociation of the polymerase holoenzyme than the DNA block (Figure 6; Table 1). Both DNA and RNA blocks increased the dissociation rate of the polymerase from the holoenzyme $30-50$-fold over the baseline rate of $0.003-0.01$ s^{-1} (*15*, *17*).

Steady-State and Stopped-Flow Measurements Using a Fluorescently Labeled Gp45 Clamp. Up to this point we have assumed that the stalled holoenzyme dissociates from the DNA. Previously, we examined the fate of the sliding clamp during holoenzyme dissociation, through the use of a fluorescence assay that employed a T7C mutant of gp45 labeled with the ANBD fluorophore, which produces a fully functional fluorescent gp45 conjugate (*17*). We have shown that dissociation of the holoenzyme from duplex DNA induces a conformational change in ANDB-45, resulting in

Table 1: Dissociation Rate Constants for Holoenzymes Complexed with Substrates Containing DNA- and RNA-17-mers[a]

	rapid quench extension assay				stopped-flow fluorescence assay	
substrate	k_{obs} (s^{-1})	F_{BL}	k_{SD} (s^{-1})	k_{BL} (s^{-1})	amplitude	k_{BL} (s^{-1})
33/62/D17	0.32 ± 0.04	0.27 ± 0.03	0.23	0.08 ± 0.03	0.031 ± 0.01	0.09 ± 0.02
33/62/R17	0.54 ± 0.1	0.38 ± 0.05	0.33	0.21 ± 0.05	0.035 ± 0.01	0.27 ± 0.04
34/62/36[b]	na[c]	na	na	na	0.028 ± 0.02	0.011 ± 0.002

[a] Assay conditions and data analysis are as described under Experimental Procedures. [b] Data from Sexton *et al.* (*17*) (used with permission). [c] Not applicable.

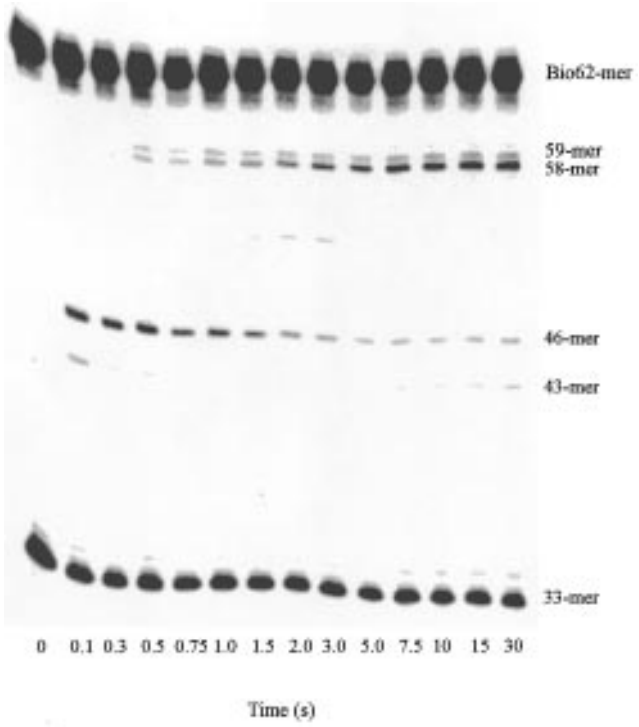

FIGURE 5: Gel electrophoresis of products from extension of the 33/62/D17 substrate, showing formation and decay of the paused products. Conditions are described under Experimental Procedures.

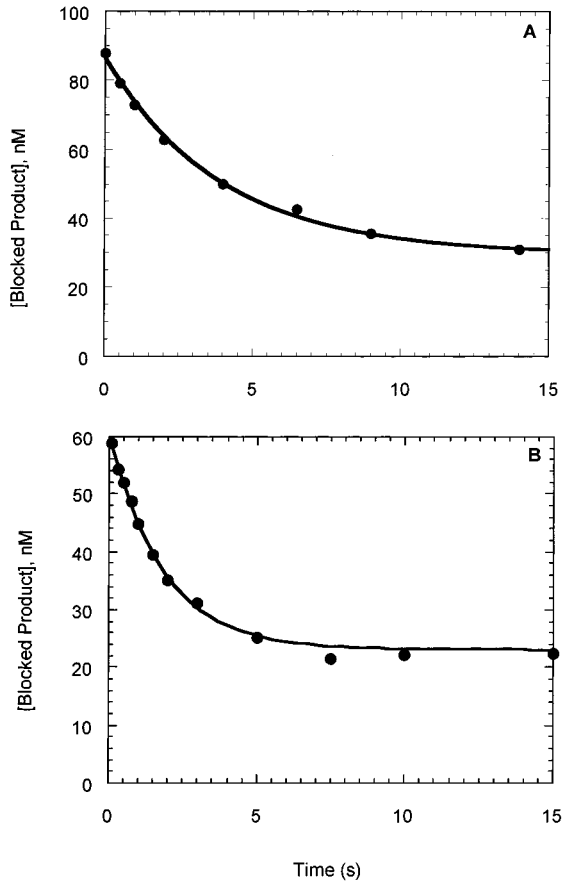

FIGURE 6: Fitted decays of intermediate products for holoenzymes on gapped substrates terminating in DNA or RNA. The substrates in each experiment were 33/62/D17 (A) and 33/62/R17 (B). Data points were collected from rapid quench time courses with the solid lines representing their fit to a single-exponential function (Experimental Procedures).

a fluorescence decrease that occurs with a rate constant identical to the weighted average of the two rate constants measured for holoenzyme dissociation by direct rapid quench kinetic analysis (0.011 s^{-1}; *4*, *17*). Given the similarity in rate constants and the fact that the polymerase·DNA complex (in the absence of gp45) dissociates with rate constants of 6−8 s^{-1} (*10*), we conclude that holoenzyme dissociation involves simultaneous departure of both the polymerase and the 45 protein.

This fluorescence assay was used in this paper to monitor holoenzyme dissociation following extension across a gap. To prevent reassembly of holoenzyme complexes in this experiment, an ATP-scavenging system was added to each sample prior to mixing. Previous tests of this scavenging system showed that it quantitatively removed ATP below the threshold required for 44/62 activity (*17*). Figure 7 shows a series of fluorescence spectra commencing with that for free ANBD-45 (spectrum 1), followed by that obtained upon addition of DNA, ATP, and gp44/62 (spectrum 2) and then polymerase addition (spectrum 3), and ending with the spectrum after gap-filling extension and depletion of ATP (spectrum 4). The magnitude of the fluorescence decrease (23%) observed following gap-filling extension by the holoenzyme is very similar to that observed earlier for holoenzyme dissociation (25%, Figure 7A). The origin of the fluorescence change detected upon completion of gap-filling extension can be assigned using the observation that the fluorescence of the ANBD-45·DNA complex was not changed upon addition of the polymerase (Figure 7A; *17*). Therefore, the observed fluorescence change is not derived form the departure of the polymerase component alone.

Using a stopped-flow instrument, we measured both the amplitude and rate of this fluorescence decrease over time for both the RNA- and DNA-blocked substrates. The amplitude associated with gap-filling extension (Table 1) matches the amplitude measured previously for holoenzyme dissociation (*17*). The first-order rate constants for the two substrates were comparable to those extracted from the strand displacement assay (Figure 7B; Table 1). For comparison, the fluorescence change over the same time period for a stalled holoenzyme on a 34/62/36-mer is shown in Figure 7B. The observed rate constants for holenzyme dissociation were greater after gap-filling extension on the blocked substrates than for dissociation of the stalled holoenzyme

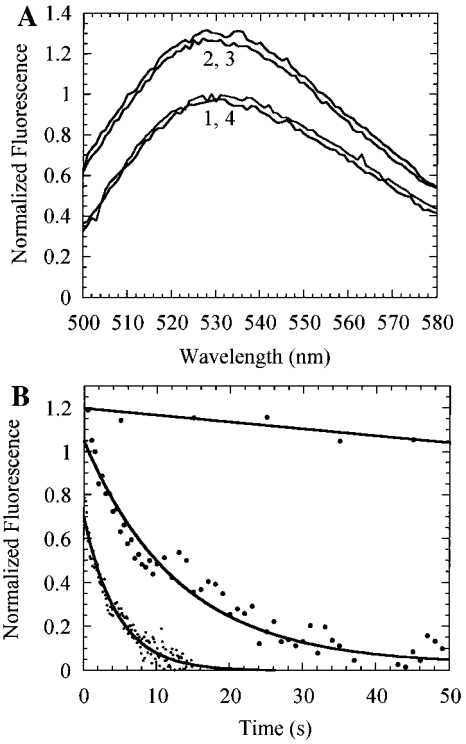

FIGURE 7: Measurements of the 45 clamp dissociation using fluorescence from a labeled cysteine mutant of 45 (T7C-ANDB): (A) Spectrum 1 shows the fluorescence emission spectrum of 45-ANDB protein in the absence of the other holoenzyme components, Spectrum 2 shows the increase in 45-ANDB fluorescence upon addition of 44/62 protein, ATP, and 33/62/D17 substrate, and spectrum 3 shows the effect of adding 43 protein to the mixture in spectrum 2. Incubation in the presence of the four dNTPS (10 μM) and an ATP-scavenging system (3 mM phosphoenolpyruvate and 10 units/mL pyruvate kinase) caused the fluorescence in spectrum 3 to decay to the level observed in spectrum 4. (B) Time courses for the fluorescence decay of holoenzyme ANDB-45·43 complexes assembled onto DNA substrates. The top curve shows the fluorescence transient observed for stalled T4 polymerase holoenzymes (45-ANDB, 44/62, and 43) assembled onto a biotinylated forked substrate (34/62/36) (*14*), the middle curve shows the fluorescence decay observed following extension of the 33/62/D17 substrate, and the lower curve shows the decay observed during extension of the 33/62/R17 substrate. The average rate constants and amplitudes are shown in Table 1. Conditions are as described under Experimental Procedures with protein and DNA concentrations at 250 nM in the presence of 1 mM ATP in 25 mM Tris-acetate, pH 7.4, 150 mM potassium acetate, and 10 mM magnesium acetate, 10 mM β-mercaptoethanol at 25 °C.

from the 34/62/36-mer (Table 1). Taken together, these results suggest that the transient fluorescence decreases we observe are due to dissociation of the polymerase holoenzyme.

Effects of Inhibition of ATP Hydrolysis and the Gp32 Protein upon Holoenzyme Dissociation. The ATP dependence of the dissociation reaction was examined by measuring the dissociation of the holoenzyme from 33/62/R17 in the presence of a large excess of ATP-γ-S, which is a potent inhibitor of the gp44/62 clamp loader activity (*23*). We found that ATP-γ-S does not affect the polymerase dissociation rate constant, k_{BL} (Table 2), suggesting that the turnover of ATP by gp44/62 complex does not play a role in this process. Likewise, the stopped-flow measurements of clamp dissociation were performed under ATP-depleted conditions, and the change in the fluorescence of the processivity clamp was monitored in the absence of ATP hydrolysis activity. It is possible that the gp44/62 complex remains associated with the holoenzyme and assists in its dissociation while binding but not hydrolyzing ATP. Clamp unloading in the *E. coli* system is catalyzed by its clamp loader and ATP-γ-S (*24*).

Table 2: Effects of Gp44/62 Inhibition and Gp32 Addition on Holoenzyme Dissociation[a]

condition	k_{SD} (s^{-1})	k_{BL} (s^{-1})
33/62/R17	0.33	0.21 ± 0.03
33/62/R17, 200 μM ATP, 2 mM ATP-γ-S	0.36	0.23 ± 0.05
33/62/D17	0.23	0.08
33/62/D17, 2 μM gp32	0.44	0.26
33/62/D17, 20 μM gp32	0.66	0.33

[a] Assay conditions and data analysis are as described under Experimental Procedures with inclusion of the indicated concentrations of the above components.

Gp32, the bacteriophage T4 single-stranded DNA binding protein, coats the DNA ahead of the lagging strand polymerase. This protein was originally known as a "helix destabilizing factor" due to its ability to passively unwind DNA (*25*). Passive unwinding by gp32 protein might be expected to promote strand displacement synthesis by the DNA polymerase, thereby effectively out-competing the dissociation reaction at the end of an Okazaki fragment and delaying termination of lagging strand synthesis. We examined dissociation of the holoenzyme·33/62/D17 complex in the presence of gp32 using the rapid quench strand displacement assay. We found that the rate constant for strand displacement, k_{SD}, did increase at higher concentrations of gp32 but that this effect was offset by a significant increase in k_{BL} (Table 2). Gp32 is known to promote quantitative strand displacement through a forked hairpin (*14*).

DISCUSSION

The bacteriophage T4 DNA replication system is an excellent model system for studying lagging strand DNA replication, because it contains only the minimal components required for continuous and discontinuous DNA synthesis. In common with prokaryotes and eukaryotes, phage T4 employs a circular processivity clamp, an ATP-dependent clamp loader, and a processive helicase/primase to prime lagging strand DNA synthesis. Although an RNase H activity is required for completion of DNA synthesis, normal cycling of the polymerase to form Okazaki fragments does not require this enzyme (*12*). Thus, a lagging strand polymerase may encounter the RNA primer from the previous Okazaki fragment as it is terminating synthesis of its current fragment. This possibility suggested that the polymerase could recognize features of the 5′ end of an Okazaki fragment that would cause the enzyme to switch from a processive to a dissociative mode. To examine this possibility, we studied the dissociation of both proteins that constitute the T4 holoenzyme, the gp43 polymerase subunit, and the gp45 processivity clamp.

On short linear substrates, the T4 holoenzyme can perform efficient strand displacement synthesis through a forked DNA substrate. A blunt-ended duplex, however, is not efficiently strand-displaced, and the holoenzyme pauses. Using a branched mechanism in which a single paused holoenzyme species can either dissociate or perform strand displacement synthesis, we calculate values for dissociation rate constants that are similar in magnitude to those measured for strand displacement. This calculated dissociation rate constant is 30−50-fold greater than the previously measured baseline

value of 0.011 s^{-1} for a paused holoenzyme, indicating that dissociation is much more efficient following extension across a gap. It is possible that topological constraints also contribute to polymerase dissociation on larger substrates, where strand displacement could be inhibited by supercoiling ahead of the DNA fork. By analogy to the increased termination observed for larger forked substrates *in vitro* (*9*), it seems likely that termination at a blunt-ended gap would be almost quantitative, because the background rate of strand displacement would be reduced.

An alternative branched pathway to Scheme 1 views the data in terms of two different species of holoenzyme·DNA complexes. The first species strand-displaces the blocking oligonucleotide, whereas the second form of the holoenzyme dissociates without preforming strand displacement. Such a mechanism raises the intriguing possibility that the two forms of holoenzyme may correspond to a processive, leading strand polymerase and a separate dissociative, lagging strand polymerase. However, no evidence for heterogeneity in holoenzyme dissociation was observed in the M13 hairpin assay used by Hacker and Alberts (*11*). Therefore, we have interpreted our time courses as reflecting the disappearance of a single enzyme species.

Given that the size of the T4 genome is 170 kb and the average Okazaki fragment length is 2 kb, there are ≈85 Okazaki fragments generated during T4 genomic replication. In the presence of gp32 we report a holoenzyme dissociation rate constant of 0.33 s^{-1} (Table 2), which corresponds to a lifetime of ∼3 s. If dissociation of the holoenzyme is required for lagging strand synthesis, then the time to process this number of Okazaki fragment is ∼4 min, which is sufficient for genomic replication (*26*). However, even a small reduction in the dissociation rate of the polymerase could cause the termination of Okazaki fragment synthesis to be rate-limiting in DNA replication. The increased strand displacement capability of the T4 holoenzyme in the presence of gp32 must be offset by an efficient termination mechanism, to prevent the polymerase from pausing or performing wasteful strand displacement synthesis. This requirement should be even more critical in eukaryotic systems in which initiation and termination of Okazaki fragments occur with a higher frequency than in prokaryotes. One factor that may trigger optimal dissociation of the lagging strand holoenzyme is its encounter with the triphosphorylated RNA tail.

However, Huang *et al*. have proposed that the 5′ terminus of an Okazaki fragment is processed by RNase H1 and RTH-1 nucleases prior to or during completion of DNA synthesis at the end of the Okazaki fragment (*27*). In this system, the terminal nucleotide could be either RNA or DNA depending upon how the processing events are ordered relative to the final gap filling synthesis step at the end of an Okazaki fragment. If RNase processing of the RNA primer occurs prior to gap-filling synthesis, then, given the relatively short time available during the elongation phase of lagging strand DNA synthesis, the processing rate must be sufficiently rapid to allow efficient recycling of PCNA and the other components of the eukaryotic lagging strand polymerase.

Summary. The bacteriophage T4 gp45 and gp43 proteins are required for both leading and lagging strand DNA replication, processes that are initiated and terminated by very different mechanisms. In lagging strand DNA synthesis, the polymerase holoenzyme must be rapidly assembled and disassembled to avoid a slowdown of the replication fork. We have shown that the T4 DNA polymerase holoenzyme is stable on a linear primer-template construct and it is able to efficiently strand displace a downstream forked oligonucleotide. When the processive holoenzyme complex encounters an RNA or DNA block, rather than a forked strand, a fraction of the holoenzyme strand displaces the block while the remainder is triggered to rapidly dissociate. A key unanswered question is the mechanism by which gp45 protein is recycled during lagging strand replication. There is no evidence that the hydrolysis of ATP by gp44/62 is important in the dissociation of the holoenzyme. This is consistent with a similar experimental result reported for dissociation in the presence of a hairpin (*11*). If all polymerase proteins are indeed conserved at the replication fork (*28*), then gp45 dissociation from the lagging strand should occur intramolecularly, such that the clamp loader immediately transfers it to the next Okazaki fragment without allowing it to escape to solution. This transfer event would require a continuous association of the clamp with some component of the replication complex. It has been suggested that gp45 slides backward across the lagging strand after Okazaki fragment termination, enabling recycling of the clamp without its dissociation from the DNA template (*14*). Our results using a fluorescently labeled sliding clamp do not support continued association of gp45 with the DNA template following polymerase dissociation, although we cannot rule out the existence of such a 45·DNA complex. Future experiments will be directed at resolving the interactions between the lagging strand polymerase and other components of the replication fork at each stage of Okazaki fragment synthesis.

REFERENCES

1. Nossal, N. G. (1992) *FASEB J. 6*, 871−878.
2. Young, M. C., Reddy, M. K., and von Hippel, P. H. (1992) *Biochemistry 31*, 8675−8690.
3. Sexton, D. J., Berdis, A. J., and Benkovic, S. J. (1997) *Curr. Opin. Chem.* Biol. (in press).
4. Kaboord, B. F., and Benkovic, S. J. (1996) *Biochemistry 35*, 1084−1092.
5. Berdis, A. J., and Benkovic, S. J. (1996) *Biochemistry 35*, 9253−9265.
6. Young, M. C., Weitzel, S. E., and von Hippel, P. H. (1996) *J. Mol. Biol. 264*, 440−452.
7. Alberts, B. M. (1987) *Philos. Trans. R. Soc. London 317*, 395−420.
8. Barry, J., and Alberts, B. (1994) *J. Biol. Chem. 269*, 33049−33062.
9. Kaboord, B. F., and Benkovic, S. J. (1993) *Proc. Natl. Acad. Sci. U.S.A. 90*, 10881−10885.
10. Capson, T. L., Peliska, J. A., Kaboord, B. F., Frey, M. W., Lively, C., Dahlberg, M., and Benkovic, S. J. (1992) *Biochemistry 31*, 10984−10994.
11. Hacker, K. J., and Alberts, B. M. (1994) *J. Biol. Chem. 269*, 24221−24228.
12. Cha, T. A., and Alberts, B. M. (1990) *Biochemistry 29*, 1791−1798.
13. O'Donnell, M. (1994) *Ann. N. Y. Acad. Sci. 726*, 153−155.
14. Hacker, K. J., and Alberts, B. M. (1994) *J. Biol. Chem. 269*, 24209−24220.
15. Kaboord, B. F., and Benkovic, S. J. (1995) *Curr. Biol. 5*, 149−157.
16. Nossal, N. G. (1979) *J. Biol. Chem. 254*, 6026−6031.
17. Sexton, D. J., Carver, T. E., Berdis, A. J., and Benkovic, S. J. (1996) *J. Biol. Chem. 271*, 28045−28051.
18. Frey, M. W., Nossal, N. G., Capson, T. L., and Benkovic, S. J. (1993) *Proc. Natl. Acad. Sci. U.S.A. 90*, 2579−2583.

19. Hinton, D., and Nossal, N. G. (1987) *J. Biol. Chem. 262*, 10873−10878.
20. Kuchta, R. D., Benkovic, P., and Benkovic, S. J. (1988) *Biochemistry 27*, 6716−6725.
21. Johnson, K. A. (1986) *Methods Enzymol. 134*, 677−705.
22. Munn, M. M., and Alberts, B. M. (1991) *J. Biol. Chem. 266*, 20024−20033.
23. Jarvis, T. C., Paul, L. S., Hockensmith, J. W., and von Hippel, P. H. (1989) *J. Biol. Chem. 264*, 12717−12729.
24. Burgers, P. M. J., and Kornberg, A. (1983) *J. Biol. Chem. 258*, 7669−7675.
25. Kowalczykowski, S. C., Lonberg, N., Newport, J. W., Paul, L. S., von Hippel, P. H. (1980) *Biophys. J. 32*, 403−418.
26. Matthews, C. K. (1994) in *Molecular Biology of Bacteriophage T4* (Karam, J. D., Ed.) ASM Press, Washington, DC.
27. Huang, Li, Rumbaugh, J. A., Murante, R. S., Lin, R. J. R., Rust, L., and Bambara, R. (1996) *Biochemistry 35*, 9266−9277.
28. Gogol, E. P., Young, M. C., Kubasek, W. L., Jarvis, T. C., and von Hippel, P. H. (1992) *J. Mol. Biol. 224*, 395−412.

BI971423P